# Rapid Communications

Projectile-charge dependence of ejected-electron spectra

V. D. Irby, T. J. Gay, J. Wm. Edwards, E. B. Hale, M. L. McKenzie, and R. E. Olson

*Laboratory for Atomic and Molecular Research and Physics Department, University of Missouri-Rolla,
Rolla, Missouri 65401*

(Received 4 January 1988)

We have studied $H^+ + He$ and $^3He^{2+} + He$ ionizing collisions at intermediate energies (60 to 120 keV/amu) and have observed a significant shift in the velocity position of the maxima in forward-ejected electron spectra when changing projectiles from protons to α particles. In ionizing collisions, a large portion of the ejected electrons are stranded near the transitory equiforce, or saddle point, position between the target ion and receding projectile. The shift in the electron spectra maxima to smaller velocities, due to changing projectiles from protons to α particles, is consistent with the shift in the saddle-point velocity when the projectile charge is increased.

In a recent paper,[1] we presented calculations and measurements of $H^+ + He$ ionizing collisions and found that ejected electrons traveling roughly midway between the two post-collision centers dominated the forward-ejection electron velocity spectra at intermediate projectile energies. This was attributed to the stranding of electrons on the transitory Coulomb equiforce, or saddle point, region between the two post-collision centers. This phenomenon can be easily visualized classically.

In this paper, we examine the effect of increasing the projectile charge on the relative position of the peak in electron velocity spectra at a forward-ejection angle of 17°. Specifically, we have investigated ionization in collisions of protons and α particles with helium at $E = 60$–120 keV/amu:

$$H^+ + He \rightarrow H^+ + He^+ + e^-, \tag{1}$$

$$He^{2+} + He \rightarrow He^{2+} + He^+ + e^-. \tag{2}$$
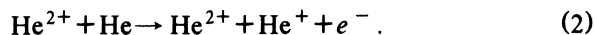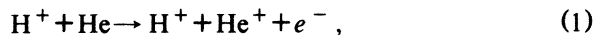
(At these energies, double electron removal is essentially negligible,[2] although we do not discriminate against it experimentally.) We present calculations and experimental data which further establish the importance of the saddle-point mechanism by illustrating the shift in electron velocity spectra due to an increase of projectile charge.

Figure 1 compares electronic potential plots for the two systems. In each case the target ion is at rest and the projectile is traveling with a speed v_p. When the charge of the projectile is increased, its Coulomb well becomes deeper and the traveling equiforce position is shifted toward the lesser charge. The velocity of the equiforce, or

saddle-point location can be shown to be

$$v_s = \frac{v_p}{1 + (q_p/q_T)^{1/2}}, \tag{3}$$

where q_p and q_T are the final charges of the projectile and target, respectively. When the projectile is changed from
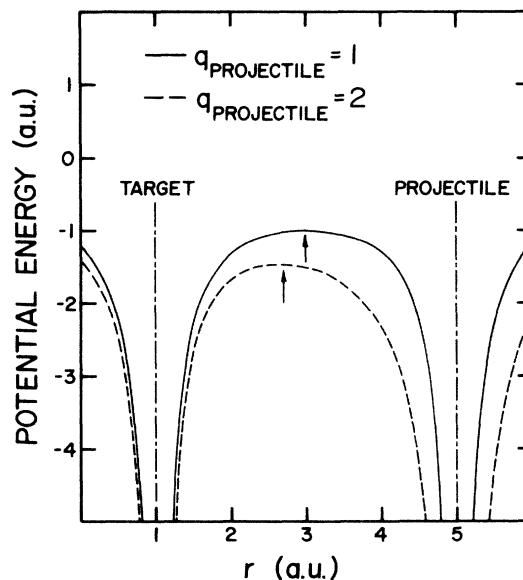

FIG. 1. Potential energy plots for $\phi = -(q_T/|1-r|) -(q_p/|5-r|)$, where q_T and q_p are the final target and projectile charges, respectively. The target is placed at $r = 1$ for convenience.

H^+ to He^{2+}, the velocity of the saddle point changes from $v_s = 0.50v_p$ to $v_s = 0.41v_p$. Since a large portion of the ejected electrons are stranded near the saddle position in ionizing collisions,[1] one would expect to observe an "inward" shift in the peak of the ejected-electron velocity spectrum when comparing α particles as incident projectiles to protons. This behavior is different than our initial naive expectation that, due to the higher charge on the α particle, the electrons would feel a stronger pull which would tend to shift the peak to a higher velocity.

To search for a saddle-point velocity shift with a helium-atom target, we have made comparisons of ejected-electron spectra for both protons and α particles with the same projectile velocities. Much of the experimental apparatus has been previously described.[1,3,4] We choose to use $^3He^{2+}$ instead of $^4He^{2+}$, due to the difficulty of electromagnetically separating $^4He^{2+}$ from H_2^+, which is abundant in the source. In order to produce adequate currents of $^3He^{2+}$, we have switched to using a microwave-ion source instead of our usual Colutron source (the maximum $^3He^{2+}$ beam current obtained with the Colutron was about 0.5 nA). The microwave source, similar to that developed by Walther, Leung, and Kunkel,[5] consisted of an 8-mm i.d. glass tube which was inserted inside a quarter-wave stub tuner. A source gas mixture of four parts ^3He and one part Ar resulted in a maximum beam current of 25 nA, with typical currents of 5 to 6 nA measured at the entrance to our target chamber.

The ion beam crossed an effusive helium target in single collision conditions. The electron-energy analyzer was of the parallel-plate type, and could be used at angles of 0°, by virtue of an aperture in the analyzer back plate, or at angles between 17° and 120°, a range dictated by analyzer and chamber geometry. The retardation and acceleration grids discussed in Ref. 3 were not used in this work. Magnetic fields in the interaction volume were reduced to less than 10.0 mG by Helmholtz coils and mu-metal shields. Possible effects due to contact potentials, electron absorption in background gas, and a neutral beam fraction were studied and shown to be negligible.

In Fig. 2, we compare typical spectra for H^+ and $^3He^{2+}$, both with the same incident velocities. An x-y recorder was used to collect the data with the x axis driven by the changing voltage across the analyzer plates, and the y axis driven by the output of a rate meter. The signal-to-noise ratio was smaller for the α particles due to lower incident beam currents. The detector efficiency function was determined by making a calibration run involving $H^+ + He$ with an incident proton energy of 100 keV, and an electron-ejection angle of 30°. This spectrum was then compared to the data of Rudd, Toburen, and Stolterfoht,[6] and the relative detection efficiency versus electron energy was obtained by dividing Rudd's data by our unnormalized cross sections obtained from the x-y plots. Calibration runs were made both before and after experimental data were taken and the detector efficiency was observed to remain constant. Beam current, chamber pressure, and rate-meter gain were recorded, and using the detector efficiency function, the relative doubly-differential cross sections were obtained by normalizing to the calibration run. Absolute cross sections were then
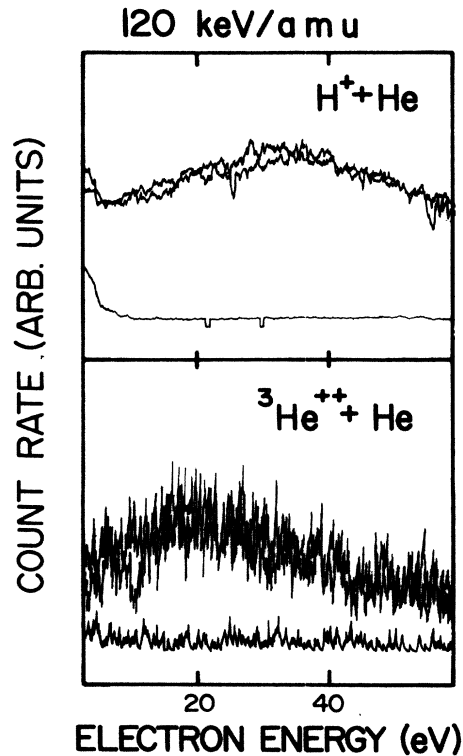
120 keV/amu

FIG. 2. Electron spectra taken for incident projectile energies of 120 keV/amu and an ejection angle of 17°. The electron energy scan is from 4 to 60 eV for both protons and α particles. The upper curves for each spectrum were taken with gas-in (chamber pressure $\simeq 2 \times 10^{-5}$ Torr uncorrected for helium); the lower curves are the gas-out background scans (chamber pressure $\simeq 3 \times 10^{-6}$ Torr).

computed by normalizing the analyzed data to the absolute cross sections reported by Rudd et al.[6] for 50 eV electrons ejected at 30° by 100-keV incident protons.

As can be seen in Figs. 2-4, there exists a significant "inward" shift of the peak in the electron velocity spectra at 60, 100, and 120 keV/amu, when the charge of the projectile is changed from 1 to 2. The shift in the electron velocity spectra corresponds to the velocity shift of the saddle point when the projectile charge is increased. We note that while the velocity of the saddle point is $0.41v_p$ and $0.50v_p$ for α particles and proton projectiles, respectively, all these data exhibit peaks at $v_e/v_p > 0.5$. The peak position is a function of projectile velocity and electron emission angle as well as the projectile charge. As the projectile velocity is increased, the relative importance of "direct," or target-centered ionization increases, and the peak shifts to a lower relative velocity (for example, the 17° electron spectrum peaks at $v_e/v_p \simeq 0.35$ for 200 keV protons in Ref. 1). The peak position does not appear to be sensitive to electron emission angle below about 10°,[4,7] but at larger angles, direct ionization begins to dominate the saddle-point contribution and the peak again shifts to lower velocities. Thus, while classical arguments based on the simple geometry of the potential saddle point are qualitatively correct, quantitative predictions must include the dynamical effects of projectile and electron velocity.

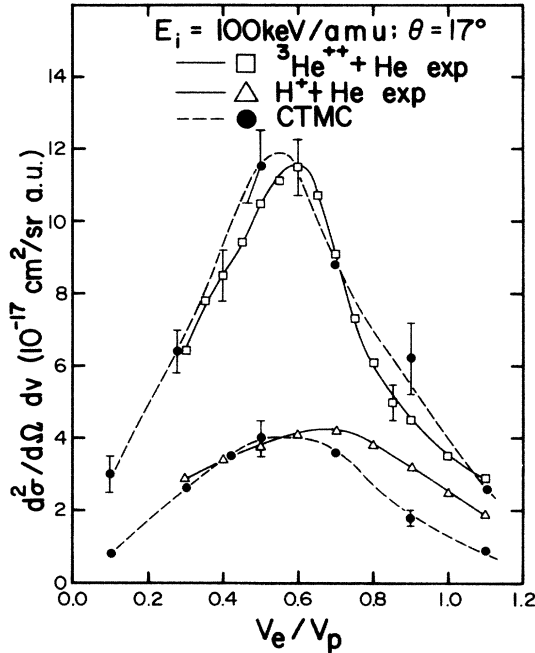In order to include these effects quantitatively, we have

FIG. 3. Doubly-differential cross sections for electron production at 100 keV/amu plotted in electron velocity space normalized to the projectile velocity. Open triangles are the proton data, and open squares are the α data. CTMC results are indicated with solid circles. Relative error for the proton data is less than 5%. Relative error for the α data is indicated. Absolute error resulting from normalization to the data of Rudd is about 25%. The dashed and solid lines serve to guide the eye.

performed classical trajectory Monte Carlo (CTMC) calculations[8,9] for reactions (1) and (2) at 100 keV/amu. The independent electron model[10] was used where the single-ionization transition probability is given by

$$P(b) = 2p_i(b)[1 - p_i(b) - p_c(b)] . \tag{4}$$

In Eq. (4), the ionization and electron-capture probabilities $p_i(b)$ and $p_c(b)$ are determined within the single-electron framework of the CTMC method. For the He atom, we used a $Z_{\text{eff}} = 1.6875$ and an ionization potential of 24.58 eV. The effects of electron capture are explicitly included in the calculations. It should be noted that for the $\text{He}^{2+} + \text{He}$ system, the coupling to ionization and electron-capture channels is quite strong, so that the $2[1 - p_i(b) - p_c(b)]$ factor of Eq. (4) varies from 0.4 at small impact parameters to 2.0 for the large impact parameter collisions.

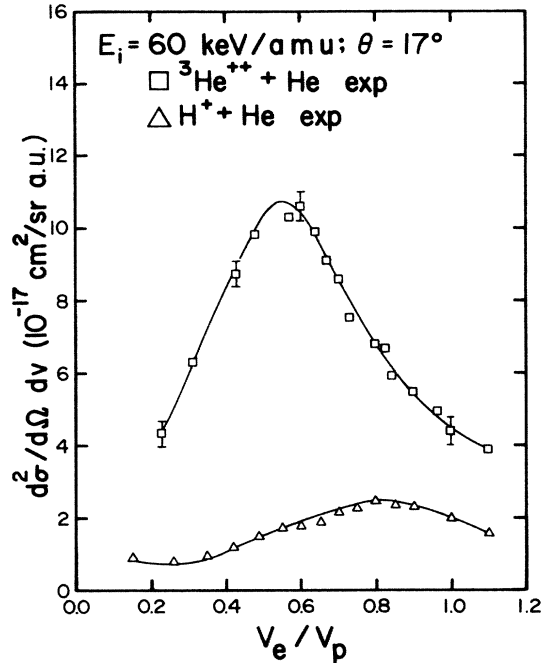We find good agreement between theory and experi-

FIG. 4. Doubly-differential cross sections for electron production at 60 keV/amu. Relative error in the α-particle data is shown.

ment (Fig. 3). The classical calculations tend to underestimate the peak positions, but there is excellent agreement in the magnitude of the doubly-differential cross sections.

In conclusion, we would like to point out the importance of making measurements at nonzero ejection angles. At $0°$, the electron velocity spectra are dominated by electrons traveling at the speed of the projectile v_p. These electrons originate from "charge capture to the continuum" (CTC) by the projectile and "wash out" the saddle-point electrons. In order to unambiguously observe the major ionization mechanisms, one has to make measurements at larger ejection angles where the CTC electrons no longer complicate the spectra. We have observed projectile charge-dependent spectra shifts at angles as high as $30°$. These shifts can be easily understood classically and are an inherent signature of the saddle-point mechanism.

[1]R. E. Olson, T. J. Gay, H. G. Berry, E. B. Hale, and V. D. Irby, Phys. Rev. Lett. **59**, 36 (1987).

[2]R. D. DuBois, Phys. Rev. A **36**, 2585 (1987).

[3]P. W. Arcuni, Ph.D. thesis, University of Chicago, 1985 (unpublished); Phys. Rev. A **33**, 105 (1986); P. W. Arcuni and D. Schneider, *ibid.* **36**, 3059 (1987). The apparatus described in these references was moved to Rolla for this work.

[4]T. J. Gay, H. G. Berry, E. B. Hale, V. D. Irby, and R. E. Olson, Nucl. Instrum. Methods (to be published).

[5]S. R. Walther, K. N. Leung, and W. B. Kunkel, Rev. Sci.

Instrum. **57**, 1531 (1986).

[6]M. E. Rudd, L. H. Toburen, and N. Stolterfoht, At. Data Nucl. Data Tables **18**, 413, (1976).

[7]D. K. Gibson and I. D. Reid, J. Phys. B **19**, 3256 (1986); Australian Atomic Energy Commission Report No. E608, 1985 (unpublished).

[8]I. C. Percival and D. Richards, Adv. At. Mol. Phys. **11**, 1 (1975).

[9]R. E. Olson and A. Salop, Phys. Rev. A **16**, 531 (1977).

[10]J. H. McGuire and L. Weaver, Phys. Rev. A **16**, 41 (1977).